11-7-2013

Effects of Cerebral Hypothermia on Cerebral Vasculature and Neuronal Activity During Pharmacologically-Induced Neonatal Seizures

Elliott James Jolly

EFFECTS OF CEREBRAL HYPOTHERMIA ON CEREBRAL VASCULATURE AND NEURONAL ACTIVITY DURING PHARMACOLOGICALLY-INDUCED NEONATAL SEIZURES

by

Elliott James Jolly

A Thesis

Submitted in Partial Fulfillment of the

Requirements for the Degree of

Master of Science

Major: Biomedical Engineering

The University of Memphis

December 2013

ABSTRACT

Jolly, Elliott James. M.S. The University of Memphis. December 2013. Effects of Cerebral Hypothermia on Cerebral Vasculature and Neuronal Activity During Pharmacologically-Induced Neonatal Seizures. Major Professors: Drs. Amy L. de Jongh Curry & Helena Parfenova.

Seizures, a common form of neurological dysfunction in newborns, occur when large groups of neurons fire in a synchronous and excessive manner. During seizures, cerebral vessels dilate to match excessive neuronal activation via increased heart rate, blood pressure, and cerebral blood flow. We hypothesized that cerebral hypothermia has beneficial neuronal, cerebrovascular, and systemic effects in neonatal seizures. Bicuculline, a $GABA_A$ receptor blocker, produces sustained seizure activity in neonatal piglets for over two hours. Electrocorticogram recordings provided no evidence that excessive neuronal activation or cerebral vasodilation were mitigated by hypothermia. These novel data suggest that cerebral hypothermia has no anticonvulsant effects and does not prevent the cerebral blood flow increase in neonatal seizures. Head cooling greatly reduced ictal tachycardia and attenuated blood pressure responses, indicating potential systemic benefits of cerebral hypothermia. Collectively, this study shows promise for the therapeutic capabilities of cerebral hypothermia during neonatal seizures.

TABLE OF CONTENTS

LIST OF FIGURES

I. INTRODUCTION

Seizures are the most common form of neurological dysfunction observed in newborns, arising from various conditions such as intracranial injuries, meningitis, asphyxia/hypoxia, metabolic disorders and neuroanatomical malformation.[1-3] The rate of incidence is approximately 3 in 1000 live births, with 80% occurring in the first week of life. Premature birth significantly increases the risk of seizure development (60-130 in 1000 live births).[4] A state of prolonged seizure activity lasting 10 minutes or greater is referred to as status epilepticus, while the clinical recurrence of this state is known as epilepsy. Often the duration of time in which epileptic seizing occurs is called the ictal period; times prior to and following these events are known as pre-ictal and post-ictal states, respectively.[1,2]

Seizing occurs when large groups of neurons fire in a synchronous and excessive manner due to an imbalance in excitatory and inhibitory neurotransmitters within the brain. The amino acid glutamate serves as a principal excitatory compound in the central nervous system (CNS).[1-3] This neurotransmitter is endogenously derived in the brain primarily from α-ketogluterate, a product of the Krebs cycle. Glutamate facilitates communication between neurons by diffusing into the synaptic space via vesicle exocytosis, where it initiates the depolarizing influx of sodium ions (Na^+) at the post-synaptic terminal.[5] The primary inhibitory neurotransmitter of the CNS, γ-aminobutyric acid (GABA), is synthesized from glutamate by the enzyme L-glutamic acid decarboxylase.[6] Like glutamate, GABA communicates its inhibitory signals through exocytosis from vesicle carriers into the synaptic gap, but instead activates the receptor $GABA_A$ which causes hyperpolarization in post-synaptic cells via chloride (Cl^-) influx. A

second receptor, $GABA_B$, increases potassium conductance, lowers calcium entry, and prevents the presynaptic release of other transmitters.[6] Actions of this compound counterbalance excitatory mechanisms present in normal neuronal behavior; if the balance between these forces is disturbed, seizures may occur.[6]

Evidence indicates that GABA has a central role in the mechanism and treatment of seizures: abnormalities in GABAergic pathways exist in both genetic and acquired animal models of epilepsy; GABA agonists surpass seizures while GABA antagonists and drugs which prevent GABA synthesis evoke them. Lastly, drugs that increase synaptic GABA are potent anticonvulsants.[6] In a study by During and Spencer, bilateral intrahippocampal microdialysis was used to examine changes in hippocampal glutamate and GABA concentrations in the conscious human brain in the preictal and ictal states. Glutamate was found to be higher inside epileptogenic hippocampal neurons while GABA concentrations were below normal. Extracellular glutamate also showed a sustained increase prior to and during epileptic events.[7] A rise in extracellular GABA was found in adjacent non-epileptogenic hippocampal neurons, suggesting that increased extracellular glutamate precipitates seizures in surrounding cells and that the concentrations reached may cause cell death.[7]

The neonatal brain is especially susceptible to these events through its abundant expression of excitatory compounds. Compared to more mature brains, the neonate has delayed maturation of inhibitory pathways and exuberant maturation of excitatory pathways.[8] These conditions create an environment that facilitates the insatiable learning patterns of the newborn and aids in establishing familiarity with the surrounding environment necessary for traditional survival.

Classifications of neonatal seizure described by Volpe are as follows: subtle (50%), clonic (25%), tonic (5%), and myoclonic (20%). Seizure types may arise in three forms: focal, multifocal and general. Focal seizures appear in an isolated region of the brain while multifocal events appear in 2 or more regions simultaneously and generalized seizures affect the entire brain. Subtle seizures are characterized by alterations in motor and autonomic functions such as ocular phenomena, oral-buccal-lingual movements, unnatural limb motion and apnea.[9] Clonic types are defined by rhythmic jerking movements of varying durations and include focal and multifocal forms. Tonic seizures consist of stiffened limb and axial muscles as well as distorted facial expressions. These seizures often last short durations of approximately 20 seconds and are more commonly generalized but may also manifest focally or multifocally in symmetrical or asymmetrical forms. Generalized tonic seizures imitate decerebrate and decorticate posturing while focal episodes do not show such behavior.[9] Myoclonic seizures are typically brief jerks and occur instantaneously, though occasionally multiple instances can occur within a short time frame.

Neonatal seizures are commonly (>50%) subclinical and require continuous monitoring via electroencephalography (EEG) in order to isolate clinical seizures.[10] Autonomic ictal manipulation from epileptic events evokes paroxysmal tachycardia, hypertension, tachypnea, increased salivation and pupillary changes in addition to transient motor dysfunction.[4] As these autonomic behaviors can be associated with numerous conditions, diagnosis is severely hindered in the absence of EEG monitoring; Health care professionals were only able to effectively isolate 27% of clinical seizures

without the aid of continuous EEG monitoring, while 73% of presumed seizures had no correlation with neuronal dysfunction.[10]

Cerebral metabolic rate (CMR) has been closely correlated with functional activity and blood flow in neural tissues on a local scale; stimulation of local neural function increases the rate of glucose utilization while decreasing this function lowers utilization rate. Changes in blood flow occur in near exact proportion to altered neuronal activity levels and resultant local glucose consumption.[11] Seizures have been associated with dramatic increases of cerebral blood flow (CBF) and heightened metabolic demands arising from excessive neuronal activation in humans and in animal models.[3] Changes in CBF were quantitatively monitored in the pre-ictal and ictal stages in the rat brain using diffusible tracers (iodo [^{14}C] antipyrine).[12] Control recordings yielded a baseline CBF of 0.86 ml/g brain/min. Readings taken at 10 and 30 minutes during the ictal period, showing values of 4.99 and 3.05 ml/g brain/min, respectively, indicating an initial increase of 580% in CBF after the first 10 minutes of seizures.[12]

To model seizure events in a laboratory setting, systemic administration of bicuculline, a $GABA_A$ receptor blocker, has been used to produce sustained seizure activity in neonatal piglets for a period of over two hours.[13] Piglets are suitable models for the neonatal central nervous system due to their comparable neuroanatomical morphology and physiology. Like human infants, piglets have a fully developed cerebral cortex at birth, which is crucial in modeling the insults observed clinically in the neocortex.[3,14]

In the newborn piglet, dilation of pial arterioles during bicuculline-induced seizures accommodates increased CBF partly through the production of carbon monoxide

(CO) via heme oxygenase (HO) activity.[3,14] Endogenous production of CO is greatly increased following epileptic seizures and in the presence of excessive glutamate concentrations, providing potent vasodilator and cytoprotective effects to neural tissues.[15] CO mediated vasodilation was shown to aid in the prevention of cerebral ischemia and glutamate excitotoxicity through elevated CBF and preservation of cerebral vascular functions after recovery from seizures.[3,14] HO activity and CO production were also directly linked to increases in neuronal activity during epileptic events evoked by bicuculline. Tin protoporphyrin (SnPP), a HO inhibitor, was shown to mitigate power in all major brainwave bandwidths (delta, theta, alpha, and beta) as well as block cerebrovascular dilation in the neonatal pig. This suggests CO could be pro-convulsant and therefore contribute significantly to the pathophysiology of epileptic seizures.[3,14]

Anti-oxidant effects of CO have been shown to prevent blood brain barrier dysfunction that arises from oxidative stress surrounding seizure events. CO can also inhibit crucial elements of oxidant-generating cellular mechanisms such as Nox4 NADPH oxidase and mitochondrial cytochrome C. This action reduces the production of reactive oxygen species and aid in the protection of cells within the brain.[15]

Decreasing CBF independently from corresponding cerebral metabolic demands results in neuronal damage and permanent cognitive impairment.[16,17] A study performed in unanaesthetized, spontaneously breathing rats investigated effects of CBF modulation during kainic-acid induced seizures. Administration of theophylline, an antagonist of the vasodilator adenosine, significantly reduced cerebral hyperaemia, prevented hyperoxia and exacerbated damage to neural tissues caused by seizure activity. This finding

suggests that increased CBF in response to seizure activity has neuroprotective properties.[18]

Electrical activity of the brain can be recorded from electrodes placed on the scalp (electroencephalography, EEG) or directly onto exposed brain surface (electrocorticogram, ECoG). EEG recording can be used in clinical situations to distinguish epileptic seizures from other types of non-epileptic seizure events and to characterize seizures for the purposes of treatment. Electrocorticograms (ECoG) are used to more effectively transduce quantitative information about neurological activity of the cerebral cortex in the peri-ictal brain. Traditional ECoGs require that the cortex be exposed via removing a section of the skull so that electrodes may be placed in direct contact with its surface. This method produces an unassisted output signal with a magnitude of millivolts (mV) as opposed to the output of microvolts (μV) obtained via EEG, providing an enhanced resolution and sensitivity for neural transduction.

Commonly measured brain activity ranges from 0.1 to 30 Hertz (Hz) and can be categorized in beta, theta, alpha and delta bandwidths based on the frequency of the wave.[13] Beta waves, 15-30 Hz, are associated with engaged conscious thought and active dreaming states. Frequencies seen during less conscious states constitute the other brain waves types, with alpha ranging from 8-14 Hz, theta from 4-7 Hz and delta below 4 Hz.[13,19] Power spectral density (PSD) analysis is a method of evaluating distribution of power in a signal over a range of frequencies. In PSD analysis, fast Fourier transforms (ffts) are commonly used to shift signals from the time domain to frequency and phase domains so that the distribution of power across a bandwidth can be assessed. PSD has been shown to accurately determine levels of brain activity in ECoGs, as it can

quantitatively assess the power of each frequency observed in both conscious and unconscious states.[20]

During seizures, blood pressure and heart rate must elevate in response to an increase in neuronal activity and cerebral metabolism.[3,13,14,21] Cerebral hypothermia (CH) by selective head cooling is thought to attenuate the hypertension and tachycardia observed during seizure, a process mediated through the parasympathetic nervous system.[16] Additionally, hypothermia was confirmed to attenuate the cerebral metabolic rate of glucose.[17] A study involving 69 neonates with moderate to severe hypoxic ischemic encephalopathy (HIE) randomly subjected infants to CH. EEG monitoring was used to assess levels of seizure activity while magnetic resonance imaging (MRI) was employed to determine extent of cerebral injury. Findings yielded lower seizure burden in infants subjected to CH with moderate HIE ($p=0.0001$) but not severe HIE ($p=0.80$). Neonates with mild ($p=0.0004$) and moderate ($p=0.02$) cerebral injury also showed decreased seizure activity while those with severe injury did not ($p=0.90$).[22]

A separate study of 45 term infants with moderate to severe HIE showed abnormal outcomes at a 12-26 month follow-up examination. Abnormal infants were more likely to have severe encephalopathy ($p=0.0002$) and clinical seizures ($p=0.03$) upon admission to the study.[23] This indicates that CH shows significant therapeutic benefit in infants only when damage to the cortex is moderate and cannot provide anti-convulsant effects in cases of extensive injury from HIE. Selective head cooling therapy has been shown to provide neuroprotective effects in HIE and is used in neonatal clinical practice as detailed above. However, central and systemic effects of head cooling during seizures in neonates have not yet been investigated.

The purpose of this study was to use the newborn pig model of epileptic seizures was to determine if cerebral hypothermia has anticonvulsant effects and can also attenuate cerebral hyperaemia, systemic hypertension and tachycardia associated with epileptic seizures. We also investigated whether head cooling alters correlation between electrical activity of the brain, cerebral vascular events, and systemic parameters during epileptic seizures. Electrical activity of the brain was measured by ECoG. Cerebral vascular events before and during seizures were measured using live cranial window microscopy by directly observing pial arterioles, the major resistance arterioles on the brain surface. Pial arteriolar diameter (PAD) is commonly used as an indicative measure of cerebral blood flow (CBF).-Systemic parameters consisting of heart rate (HR), mean arterial pressure (MABP), and core body temperature (T) were recorded to assess the levels of tachycardia and hypertension during seizures. All central and systemic parameters were recorded and analyzed in two groups of newborn piglets, control group, and head cooling group, before and during bicuculline-induced seizures.

II. METHODS

A. Preparation

Piglets 3-7 days old (n=26) were sedated and anesthetized using intramuscular injection of ketamine (33 mg/kg) and xylazine (5 mg/kg) in an animal holding facility. Piglets were then transported to the lab for surgical preparation. The arms and legs of the animal were secured with paper tape and instrumentation for the procedures was connected. Manual stimulation of the corner of the piglet's eye or the bottom of the piglet's foot was used to confirm complete unconsciousness.

Catheters were inserted into the femoral artery and vein for intravenous delivery of chemical agents and recording HR and MABP. A blood sample was taken and gas levels were analysed at this time to determine if adjustments were necessary. A tracheal tube was inserted to regulate respiration via mechanical ventilation. Once all above steps were complete, the animal was placed on a servocontrolled heating pad and secured in a stereotaxic unit. Bilateral ear bars were guided through the tympanic membrane and into the temporal bone of the skull to stabilize the animal and prevent motion artifacts. A digital thermal probe was inserted into the rectum of the animal to monitor core body temperature during the experiment. Blood gas levels were then adjusted to a normal range (P_{O2}: 90 mmHg, P_{CO2}: 40 mmHg, pH: 7.45) Additional readings were often required to ensure gas levels were achieved and maintained.

B. Electrocorticogram (ECoG) recordings

In order to acquire ECoG data, two stainless steel screws were placed in the right hemisphere of the parietal bone to serve as electrodes. Screws 10 mm in length were

placed 2.5 cm apart, each penetrating the skull approximately 4 mm to contact the underlying dura mater. A differential amplifier (DAM 50, World Precision Instruments) was first attached to a waveform generator to assess the performance of the device. Gain was set to 1000. Data were converted from analog to digital form with a cDAQ system (model 9172, National Instruments) and recorded at a rate of 250 Hz using LabVIEW 2011 (National Instruments). To test the gain of the amplifier, a short segment of 10 Hz signal was recorded, the amplifier was detached and the waveform generator was recorded unassisted at the same output for experimental gain calculation. Alligator clamps were used to attach both leads to the screws and a reference electrode was placed on the tongue of the animal. The amplifier was then connected to obtain a single differential ECoG signal from the two skull electrodes.

C. Cranial window intravital microscopy

Experiments which recorded changes in PAD required placement of a cranial window in the left hemisphere of the skull. This device consisted of a glass window housed in a metal ring with three injection sites located around its perimeter for the replacement of periarachnoid cerebrospinal fluid (pCSF). After piglets were secured in a stereotaxic unit, the scalp and cranial periosteum were removed with a scalpel to prepare the skull for the cranial window. Any damaged vessels on the surface of the skull were allowed to clot at this time. If bleeding persisted, wax was applied to prevent blood from pooling in the surgical site. An outline of the cranial window was traced onto the skull and bone was carefully removed using curved-tipped rongeurs. The dura mater was peeled away with care to avoid tearing the cerebral cortex; bleeding from the brain has

the potential to cloud the cranial window and compromise data acquisition. Once the dura was removed, dental acrylic was used to secure the window in place. Finally, artificial cortical cerebrospinal fluid (aCSF) (in mM: 3.0 KCl, 1.5 MgCl2, 1.5 CaCl2, 132 NaCl, 6.6 urea, 3.7dextrose, and 24.6 NaHCO3, pH 7.4) was injected into the cavity below the window.

D. Experimental data acquisition

For the initial ECoG study, baseline activity was recorded for 30 minutes prior to seizure induction. Systemic parameters (HR, MABP, T) were documented in a laboratory notebook in 5-minute intervals before and during seizures. Core body temperature was assessed via the digital display of the rectal thermometer. HR and MABP were transduced from the femoral artery in real time and continuously displayed on an ECG monitor (Model #90623A, Spacelabs). Piglets were placed on a servocontrolled heating pad throughout the experiment. A camera fixed in a stereotaxic unit was used to continuously capture PAD from the cranial window. Video signal was fed into a display monitor where calibrated lines were utilized to determine the diameter of large and small arterioles. One larger diameter arteriole (70-100 μm) and one small arteriole (40-60 μm) were observed during each experiment. All data were recorded in a laboratory notebook.

E. Experimental protocol

Baseline data for all experimental parameters were gathered in 5 minute intervals for a total of 30 minutes after piglets were prepared and stabilized. Intravenous administration of the paralytic pancuronium bromide (0.5 mg/kg, Sigma Aldrich)

occurred 5 minutes prior to seizure induction to inhibit muscular activity and prevent resultant motion artifacts from compromising data acquisition. Once the paralytic fully took effect, intravenous injection of 3 mg/kg bicuculline (Tocris), a $GABA_A$ antagonist, was performed to induce seizures. All central and systemic recordings were continued for the 2-hour period following seizure onset. At the end of this time period, potassium chloride (KCl) was administered intravenously to euthanize the piglet. ECoG was recorded for approximately 5 minutes after death occurred.

F. Experimental groups

Piglets in the control group (n=13) underwent two hours of bicuculline-induced seizure activity following baseline recordings and received no therapeutic intervention during this time. Animals in the CH (cooled) group (n=13) were subjected to localized hypothermia throughout the two hours of seizure activity. To cool the head without obscuring the view of pial arterioles through the cranial window, specialized ice packs were created by placing a hole of equal size in the center of a resealable plastic zip-lock type bag. Material of the ice pack was resealed with heat after the hole was formed. For experiments utilizing CH, cooling was initiated 30 minutes prior to bicuculline administration by placing specialized ice packs in direct contact with the temporal and occipital regions of the head. Ice packs were changed approximately every 45 minutes throughout application. Heating pads were used as needed to maintain core temperature inside a range of 35-37.5 ºC and ensure systemic hypothermia was not reached.

G. Data analysis

ECoG signals were assessed using MATLAB R2011a (MathWorks). Spike frequency (n=12), ECoG amplitudes (n=12), and power spectral density (PSD) (n=12) were derived from the raw data signals. These ECoG parameters were averaged in 5 minute time blocks for correlation with other experimental parameters. Histograms of spike amplitude distribution were also constructed in order to better visualize the variation in spike amplitudes in each group.

For spike frequency, signals were parsed into 10 data point (0.04 s) windows where the algorithm calculated mean, standard deviation, maximums and minimums of ECoG amplitudes. To detect seizure spikes, the standard deviation of the current 10 data point set was calculated and compared to a threshold value derived from the standard deviation of the respective recording's baseline activity. If the standard deviation surpassed threshold, spike count was incremented for the respective 5 minute time block. This threshold comparison method was verified through correctly locating all spikes within sample segments of ECoG signals with known numbers of seizure spikes.

A Boolean operator was used to denote when the signal had entered a seizure state to prevent multiple increments from a single spike. As seizure spikes were often more than one window in length, it was necessary to retain maximums and minimums across multiple window segments in order to determine extrema for each seizure spike. After the initial encounter with an instance of seizure spike, the signal was parsed window by window until the algorithm encountered a segment with a subthreshold standard deviation.

Maximums and minimums from the current 10 data point set were compared to the spike's overall maximum and minimum values at each window between first and last suprathreshold segments. Upon the return to subthreshold standard deviation, parameters for the spike were then stored and the Boolean operator was reset. At the end of each 5 minute time block, spike count values were divided by the amount of elapsed time and recorded as average number of spikes per second.

Amplitudes for histograms were calculated by subtracting each spike's maximum and minimum values. Bins in which amplitude frequency was stored ranged from 0 to 3.5 mV in 0.25 mV increments. Upon the return of standard deviation to a subthreshold level, the value for amplitude was compared to the bin range and the proper bin was incremented for the current 5 minute segment. Once signal analysis was complete, histogram output was first condensed into 20 minute segments by summing total spikes in each bin across all time points within the specified time block. These values were then used to calculate representative means for each experimental group. Initial data points post-seizure induction were also analysed individually to gain an understanding of behaviour immediately following bicuculline administration.

ECoG amplitudes were found by analyzing signals in 5 minute blocks using a MATLAB algorithm. The five-minute blocks were broken into 30 separate 10 second windows consisting of 2500 data points each. Maximum and minimum values inside the window were determined and stored in temporary variables. As described by Daley, et al., the 10 second window was again analyzed to average all amplitudes within 5% of the current extrema to establish mean peak for the window. This value was found by taking the difference between averaged maximums and minimums. When the end of a 5 minute

time block was reached, mean peaks were averaged together to represent the overall average amplitude. Representative means and standard deviations were calculated for each experimental group by averaging 5 minute blocks from each animal. Standard deviation and standard error of the mean (SEM) were also derived from these values, the SEM serving as error bars for graphical comparisons.

PSD analysis was performed via fast Fourier transform (fft) with a temporal resolution of 10 seconds and a frequency resolution of 0.1 Hz. The length of the fft output array was proportional to the temporal resolution multiplied by the sampling rate (t*fs). This array was then cut in half length-wise to eliminate duplicate points and the absolute value was taken so that the frequency spectrum could be plotted. The resulting array was then scaled by dividing each value by the length of the original vector to conserve power. To calculate the power spectrum, values in the array had to be squared to be converted from the frequency spectrum. Finally, since half of the output vector was dropped, it was necessary to multiply each entry by 2 to conserve energy of the output.

Representative means from each experimental group were calculated for each 5 minute time block. A range of 0-30 Hz was examined by summing values of a specific frequency and its surrounding 1 Hz range, e.g. 1±0.5 Hz. Single Hertz values were condensed into cognitive bandwidths extending from delta to beta in order to simplify visualization of the data. These values were then expressed as a percentage of baseline activity to normalize observed increases in power after seizure induction. Thirty minute segments of non-seizure data were used to determine average baseline values. Both baseline and seizure data were calculated in units of power (V^2). SEM was used to form the error bars for individual entries on a bar chart made for comparison.

PSD data from seizure activity was used to compare levels of cognitive processes between experimental groups. The data was divided into 20 minute segments and percentage increase of baseline power output was compared over a range of frequencies. F-tests were used to determine if variances were equal between frequencies at each respective time point. Appropriate t-tests were performed at $\alpha = 0.05$ significance level.

Systemic and PAD data from both groups were assessed to investigate significant differences among cooled and control groups. Heart rate (bpm), mean arteriolar pressure (mmHg) and temperature (ºC) data were used to find respective arithmetic means for the parameters. Changes were graphed over time for comparison among groups. SEMs were employed in charts as error bars. Statistical testing was performed at $\alpha = 0.05$ significance level for each 5 minute time block to uncover any significant differences among groups.

Values for PAD of both small (30-60 μm) and large (70-100 μm) arterioles were expressed as a percentage of increase in baseline activity. The ratio of measurements from 5 minute time blocks to each animal's respective baseline diameter was found and expressed as a percentage. Baseline diameter was taken from the initial reading made at 40 minutes prior to bicuculline administration for each data set. Percentage increases from each animal were used to compile representative means for both experimental groups. SEM for each time point was used to construct the error bars for individual entries on a bar chart made for comparison between groups. T-tests were performed on contiguous 5 minute time segments, comparing the average values from each group for each time segment. Correlation coefficients were also calculated for each possible pair of parameters among systemic, PAD and ECoG data, in one hour segments and half hour segments.

H. Statistics

F-tests were performed on data points from each parameter and it was determined that a large majority of points did not have equal variances. Data from each experimental group was compared in all of the above parameters using Welch's t-test for samples of unequal variance. Each five-minute time point tested over the duration of the experimental time frame had separate means and standards deviation associated with each group. Sample sizes were constant for each parameter. Degrees of freedom for individual tests were calculated using the Welch-Satterwaite equation.[24]

III. RESULTS

A. Effects of head cooling on core body temperature

Values of temperature at each five minute time segment were averaged independently for both groups and plotted over time to illustrate thermal deviation (Fig. 1). Head cooling significantly lowered the core temperature of CH animals for the entirety of the experiments.

B. Effects of head cooling on electrical activity of the brain before and during seizures

The transition from normal neurological behavior to seizure state (Fig. 2) is made up of seizure spikes that increase in frequency until an intense, chaotic pattern emerges. This chaotic behavior is pronounced throughout the early ictal state. Example ECoG recordings for both cooled and control animals are displayed in Fig. 3, A-D. Injections times for bicuculline and potassium chloride (KCl) are denoted on each graph. Values for mean ECoG amplitudes and spike frequency are shown in Figs. 4 A & B respectively.

Head cooled animals showed significantly higher amplitudes (Fig. 4A) than the control group ($p < 0.05$ for 15 min and the75-90 min interval), but seizure spikes per second (Fig. 4B) were similar among groups over all time points.

C. Seizure spike amplitude distribution analysis

Similar to ECoG amplitude analysis, data sets from simultaneous PAD and ECoG investigations were discarded from seizure spike amplitude distribution means. The distribution of spike amplitudes over the first 30 minutes of post-bicuculline seizure state was considered at individual 5 minute time points. This was done to further understand

the changes that occurred during the initial intense reaction to bicuculline and to observe any differences caused by head cooling. Histograms containing these comparative data are located in figures 4A-4F below.

Statistical analysis was performed as outlined in the Methods section above and resulting probabilities are listed in Table 1. The time frames of 10-15 minutes and 25-30 minutes of seizures have significant differences in their distribution between normothermic and head cooled piglets. Cooled animals show a lower number of spikes in lower amplitudes ranging from 0.75-1.25 mV for the 10-15 minute block when compared to control normothermic piglets (Fig. 5C). The period of 25-30 minutes also possesses significantly different spike distribution, with cooled animals exhibiting a greater number of spikes in the 2.25-2.75 mV range (Fig. 5F).

Comparative histograms of spike amplitude distribution were also constructed for 20 minute intervals throughout the two hour seizure period (Figs. 6 A-F). Probability values for these comparisons are listed in Table 2. We evaluated spike amplitude distributions over 20 minute intervals for the overall 120 minute duration of seizures (Table 2, Fig. 6). Statistical evaluation of spike amplitude histograms revealed that distributions for the final 40 minutes were significantly different among groups. Higher amplitude (1-2.5 mV) bins were consistently greater in cooled piglets for 85-100 minute and 105-120 minute windows (Table 2). Observations in both initial and long-term analysis suggest that cooling increases voltage output of cortical activity during late ictal periods (80-120 minutes).

D. Assessment of 20 minute PSD segments

Cognitive bandwidths ranging from low delta to beta (0.1-30 Hz) were used to condense PSD output into histograms for comparison among CH animals and controls. Histograms are shown in Figure 7 below. We found no statistically significant differences between cooled and control groups (Table 3). However, throughout the majority of the 2 hour ictal period, cooled animals showed a frequency distribution weighted towards higher bandwidths, with delta increasing in the later ictal period (80-120 min). In contrast, controls had more activity in lower bandwidths (1-14 Hz), the highest activity being in alpha waves (Fig. 7A-F).

E. Effects of head cooling before and during seizures on systemic parameters

Values of HR and MABP from each group were averaged for each five minute time segment and graphed for comparison. Though head cooling did not significantly reduce HR during the baseline period 30 min before seizure induction, CH significantly lowered HR for the entire seizure period (Fig. 8A). We did not find any statistically significant changes in MABP in response to head cooling before or during seizures, although the trend of the cooled group's MABP during 10-90 min of the ictal period appears to be lower than in the control group.

F. Effects of head cooling before and during seizures on pial arteriolar diameter

The diameters of small (40-60 μM, Fig 9A) and large (70-100 μM, Fig. 9B) pial arterioles were recorded. Seven piglets were used in each group, each only contributing one large and one small arteriole to the study. Dimensions of PAD recorded during

experiments were expressed as percent of the baseline diameter for its respective arteriole to normalize haemodynamic responses among experimental animals (Fig. 9).

Ice packs were placed on the animals half an hour prior to bicuculline administration in order to acquire baseline CH responses. Observing the effects of CH on baseline PAD shows that there was no significant difference between controls and cooled animals in small or large vessels prior to seizure onset. Following bicuculline injection, PAD recordings in CH animals returned to baseline more quickly than controls, particularly in small PAD measurements (Fig. 9A,B). It appears that the vasodilator responses of small arterioles to seizures are greater than the responses of larger arterioles. Smaller arterioles show a greater difference among controls and cooled groups than that of large arterioles, though these changes are not statistically significant.

IV. DISCUSSION

We established an experimental model and developed techniques necessary to investigate the effects of head cooling on electrical activity of the brain, cerebral vascular events, and systemic parameters during epileptic seizures. Furthermore, we collected novel data suggesting that head cooling has no anticonvulsant effects in the bicuculline model of neonatal seizures. ECoG data provided no evidence that seizure activity was mitigated by hypothermia in either neural firing rate or cognitive bandwidth activity. PSD data indicated groups were not statistically different despite distinct observable differences in distribution trends; probabilities were near the level of significance for multiple points of PSD analysis. In contrast, ECoG amplitudes were increased in response to application of hypothermia, suggesting heightened neural output occurs. This observation was reinforced by spike amplitude distributions, as controls have fewer high amplitude spikes than CH animals while overall spike counts are similar.

The implications of this difference in neural output could be interpreted to mean cerebral hypothermia has pro-convulsant properties. However, without additional evidence to support this hypothesis, it is difficult to conclude that head cooling exacerbates seizure activity. In other circumstances, CH has been shown to reduce cerebral metabolic rates and attenuate seizure burden, neither of which seem to indicate pro-convulsion. These facts help rationalize that the observed difference in ECoG amplitudes may be systematic in origin. Still, there may be underlying physiological processes responsible for some if not all of this change in behavior. In future studies, control tests or precautionary measures should be taken to eliminate this discrepancy.

Our data shows that head cooling has beneficial effects in systemic circulation by reducing tachycardia during the ictal period. Heart rate peaked at lower magnitudes and re-established basal values in cooled animals during the ictal period, where controls showed elevated heart rates throughout. Blood pressure and pial arteriole dilation remained relatively unchanged according to our data, though differences may become significant if sample size were increased. Statistical probabilities for both PAD parameters, particularly small diameter vessels, were commonly below 15%. The ability of CH to mitigate these behaviors reflects its ability to alleviate hyperaemia.

As CH is well known for its ability to reduce cerebral metabolism, it is reasonable to assume that experimental animals underwent a similar response. However, metabolism was not directly measured in this study, thus we cannot ascertain if the observed decrease in heart rate is disproportional to any decrease in cerebral metabolic rate experienced during the ictal period. There were no significant changes in blood pressure or dilation of pial arterioles, thus it is inferred that CH does not alter these physiologic pathways in the bicuculline model. Heart rate is the only factor measured in this study that contributed to a reduction in CBF, making the scenario where blood flow is uncoupled from metabolically charged neurons seemingly less probable. It would be beneficial to observe metabolism and blood flow directly in future studies in order to determine the relationship in these parameters in the presence of hypothermia.

Collectively, this data shows promise for the therapeutic capabilities of cerebral hypothermia during neonatal seizures. Despite an absence of statistical significance, many of the parameters tested were observably lower in cooled animals, suggesting that a benefit exists and can be elucidated through continued research. Measurements of blood

flow and cerebral metabolism would prove informative when assessing the relationship between attenuated CBF and metabolic demands of hyperactive neurons. Additionally, the administration of a range of bicuculline concentrations may be of interest to determine the effects of head cooling during less severe instances of status epilepticus.

V. CONCLUSION

We established an experimental model and developed techniques necessary to investigate the effects of head cooling on electrical activity of the brain, cerebral vascular events, and systemic parameters during epileptic seizures. In newborn piglets, head cooling produces a rapid and sustained decrease in core body temperature to 34-35º C. Our novel data demonstrate that head cooling has no anticonvulsant effects in the bicuculline model in newborn piglets. In contrast, increased ECoG amplitude in cooled piglets indicates the potential of pro-convulsive contribution. Power spectral density analysis yielded no statistical difference among normothermic and head cooled groups Head cooling had beneficial effects in systemic activity by reducing tachycardia during the ictal period. Collectively, this study shows promise for the therapeutic capabilities of cerebral hypothermia during neonatal seizures.

REFERENCES

1. Rose A, Lombroso C. Neonatal seizure states - A study of clinical, pathological, and electroencephalographic features in 137 full-term babies with a long-term follow-up. *Pediatrics*. 1970; 45(3): 404-425.

2. Ziburkus J, Cressman J, Schiff S. Seizures as imbalanced up states: Excitatory and inhibitory conductances during seizure-like events. *J Neurophysiol*. 2013; 103(5): 1296-1306. DOI: 10. 1152/jn.00232.2012.

3. Carratu P, Pourcyrous M, Fedinec A, Leffler C, Parfenova H. Endogenous heme oxygenase prevents impairment of cerebral vascular functions caused by seizures. *Am J Physiol Heart Circ Physiol.* 2003: 285(10): 1148-1157. DOI: 10.1152/ajpheart.00091.2003.

4. Panayiotopoulos C. *The Epilepsies: Seizures, Syndromes and Management.* Oxsfordshire, UK. Bladon Medical Publishing. 2005.

5. Marks L, Prosta R, Ulmers J, et al. Pictorial Review of Glutamate Excitotoxicity: Fundamental Concepts for Neuroimaging. *AJNR* 2001: 22: 1813-1824. PMID: 11733308.

6. Treiman D. GABAergic Mechanisms in Epilepsy. *Epilepsia.* 2001: 42(3): 8-12. DOI: 10.1046/j.1528-1157.2001.042suppl.3008.x.

7. During M, Spencer D. Extracellular hippocampal glutamate and spontaneous seizure in the conscious human brain. *The Lancet*, 341(8861): 1607-1610. PMID: 8099987.

8. Wyllie E, Gupta A, Lachwani D. *The Treatment of Epilepsy: Principles and Practice.* Philadelphia, PA. Lippincott Williams & Wilkins. 2006.

9. Volpe J. Neonatal Seizures: Current Concepts and Revised Classification. *Pediatrics.* 1989: 84(3): 422-428. PMID: 2671912.

10. Chapman K, Raol Y, Brooks-Kayal A. Neonatal Seizures: controversies and challenges in translating new therapies from the lab to the isolette. *European J. of Neuroscience.* 2012: 35(10): 1857-65. DOI: 10.1111/j.1460-9568.2012.08140.x.

11. Sokoloff L. Relationships among local functional activity, energy metabolism, and blood flow in the central nervous system. *Fed Proc.* 1981 Jun; 40(8): 2311-6. PMID: 7238911.

12. Horton R, Meldrum B, Pedley T, McWilliam J. Regional cerebral blood flow in the rat during prolonged seizure activity. *Brain Research.* 1980: 192(2): 399-412. PMID: 6769547.

13. Parfenova H, Daley M, Carratu P, Pourcyrous M, Leffler C. Heme Oxygenase inhibition reduces neuronal activation evoked by bicuculline in newborn pigs. *Brain Research.* 2004: 1014(2004): 87-96. PMID: 15212995.

14. Parfenova H, Carratu P, Tchereanova D, Pourcyrous M, Fedinec A, Leffler C. Epileptic seizures cause extended postictal cerebral vascular dysfunction that is prevented by HO-1 overexpression. *Am J Heart Circ Physiol.* 2005: 288(10): 2846-2850. DOI: 10.1152/ajpheart.01274.2004.

15. Leffler C, Parfenova H, Jaggar J. Carbon monoxide as an endogenous vascular modulator. *Am. J. Phys. – Heart and Circulatory.* 2011: 301(10): H1-H11. DOI: 10.1152/ajpheart.00230.2011.

16. Nakashima K, Todd M, Warner D. The relation between cerebral metabolic rate and ischemic depolarization: A comparison of the effects of hypothermia, pentobarbital, and isoflurane. *Anesthesiology*. 1995; 82(5): 1199-1208. PMID: 7741295.

17. Busila D, Leffler CW. Hypothermia reduces cerebral metabolic rate and cerebral blood flow in newborn pigs. *AJP - Heart*. 1987; 253(4): H869-H873. PMID: 3661735.

18. Pinard E, Riche D, Puiroud S, Seylaz J. Theophylline reduces cerebral hyperaemia and enhances brain damage induced by seizures. *Brain Research.* 1990: 511(2): 303-9. PMID: 2334848.

19. Dunn B, Hartigan J, Mikulas W. Concentration and mindfulness meditations: Unique forms of consciousness. *Appl Psychophysiol Biofeedback*. 1999; 24(3): 147-165. PMID: 10652635.

20. Glass A, Kwiatkowski A. Power spectral density changes in the EEG during mental arithmetic and eye-opening. *Psychologische Forschung.* 1970; 33(2): 85-99. PMID: 5515904.

21. Perlman J, Volpe J. Seizures in the preterm infant: Effects on cerebral blood flow velocity, intracranial pressure, and arterial blood pressure. *The Journal of Pediatrics*. 1983; 102(2): 288-293. PMID: 6822940.

22. Srinivasakumar P, Zempel J, Wallendorf M, et al. Therapeutic Hypothermia in Neonatal Hypoxic Ischemic Encephalopathy: Electrographic Seizures and Magnetic Resonance Imaging Evidence of Injury. *Journal of Pediatrics.* 2013: 01(041): 1010-1016. DOI: 10.1016/j.jpeds.2013.01.041.

23. Takenouchi T, Cuaycong M, Ross G, et. al. Chain of Brain Preservation—A concept to facilitate early identification and initiation of hypothermia to infants at high risk for brain injury. *Resuscitation.* 2010: 81(12): 1637-41. DOI: 10.1016/j.resuscitation.2010.08.001.

24. Wang Y. Probablities of the Type I Errors of the Welch Tests for the Behrens-Fisher Problem. *Journal of the American Statistical Association.* 1971: 66(335): 605-8. DOI: http://www.jstor.org/stable/2283538.

APPENDIX

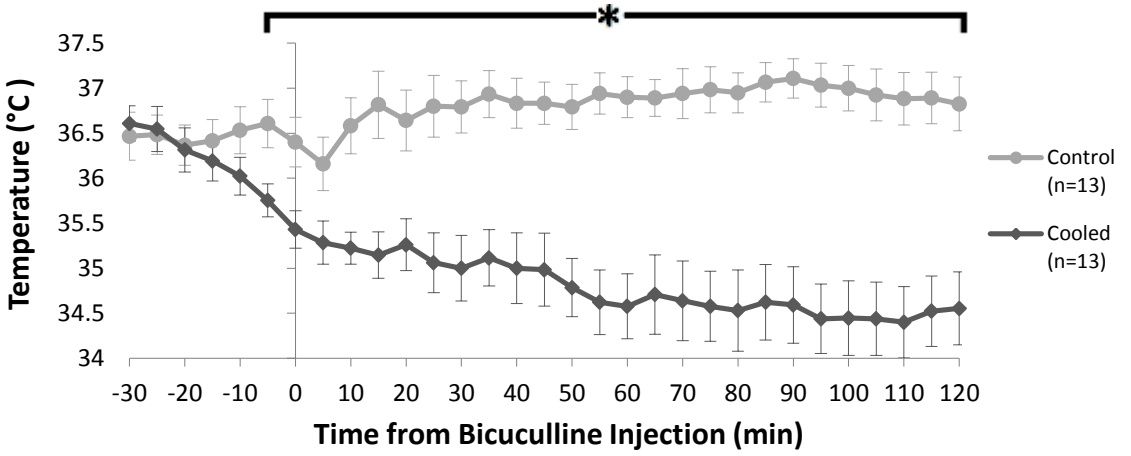

Figure 1. Effects of head cooling on core temperature before and during seizures. Values are means ± SE. * p<0.05.

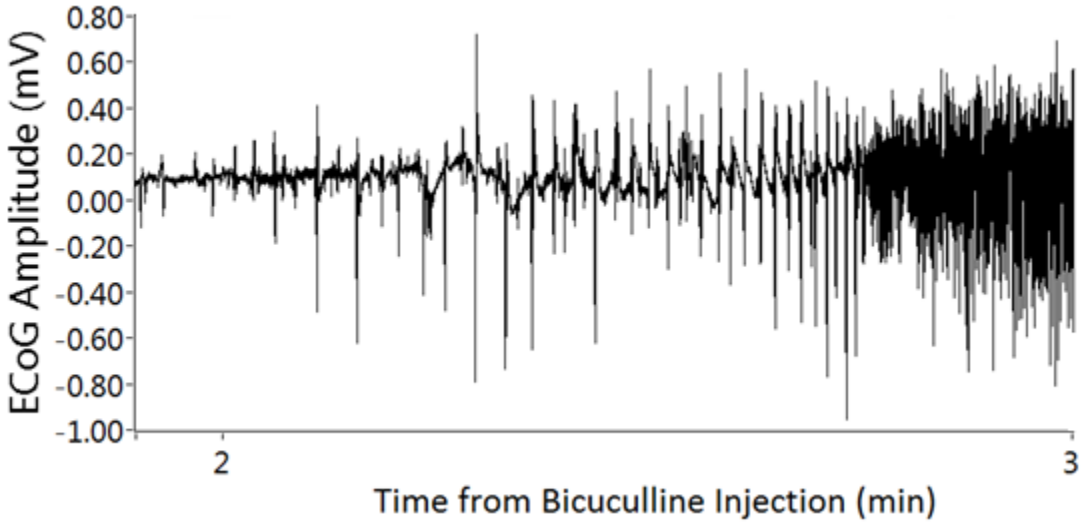

Figure 2. Example of transitional period between normal neurological behavior and seizure state.

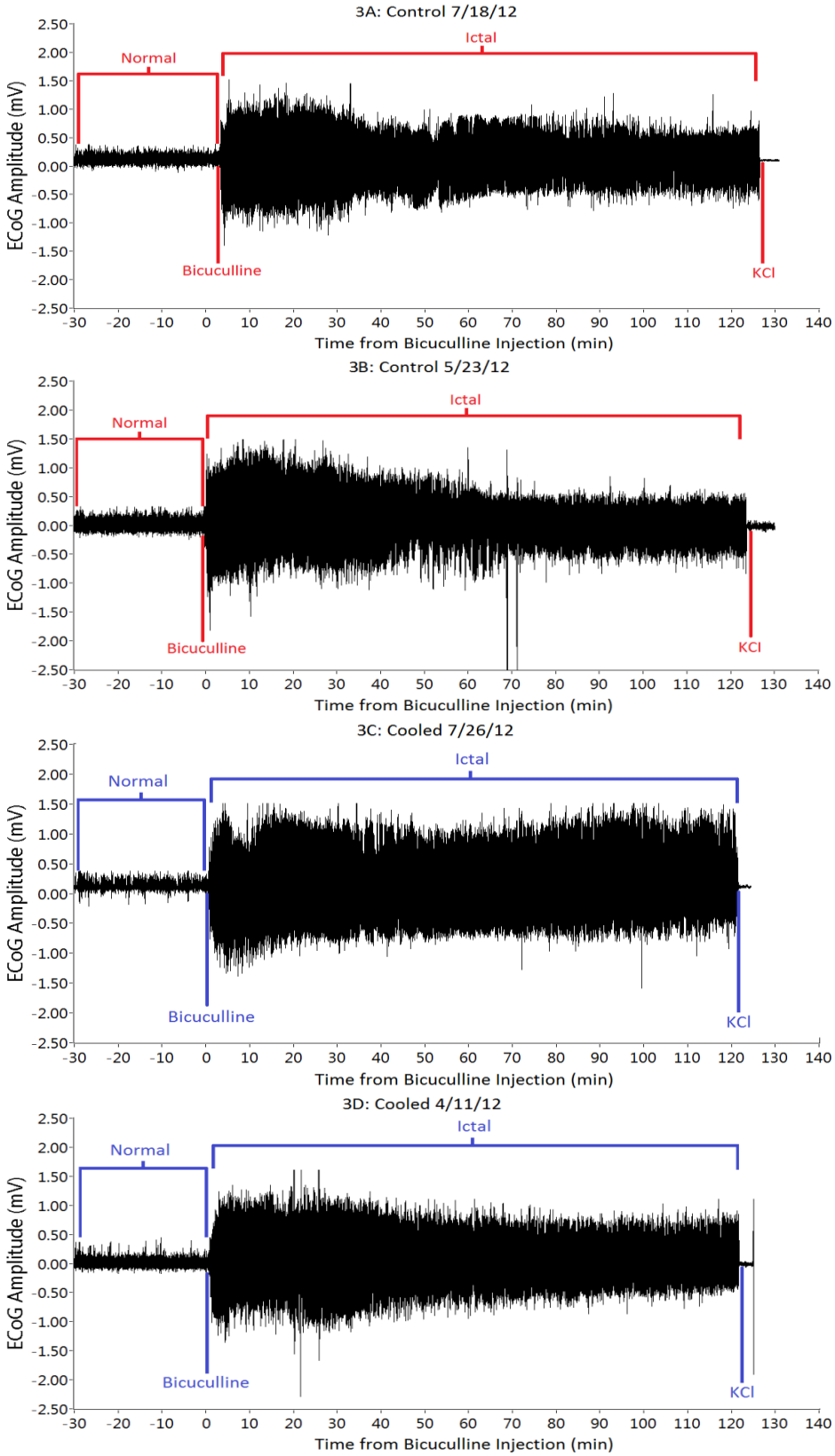

Figure 3. Example ECoG recordings from control (A, B) and cooled (C, D) animals.

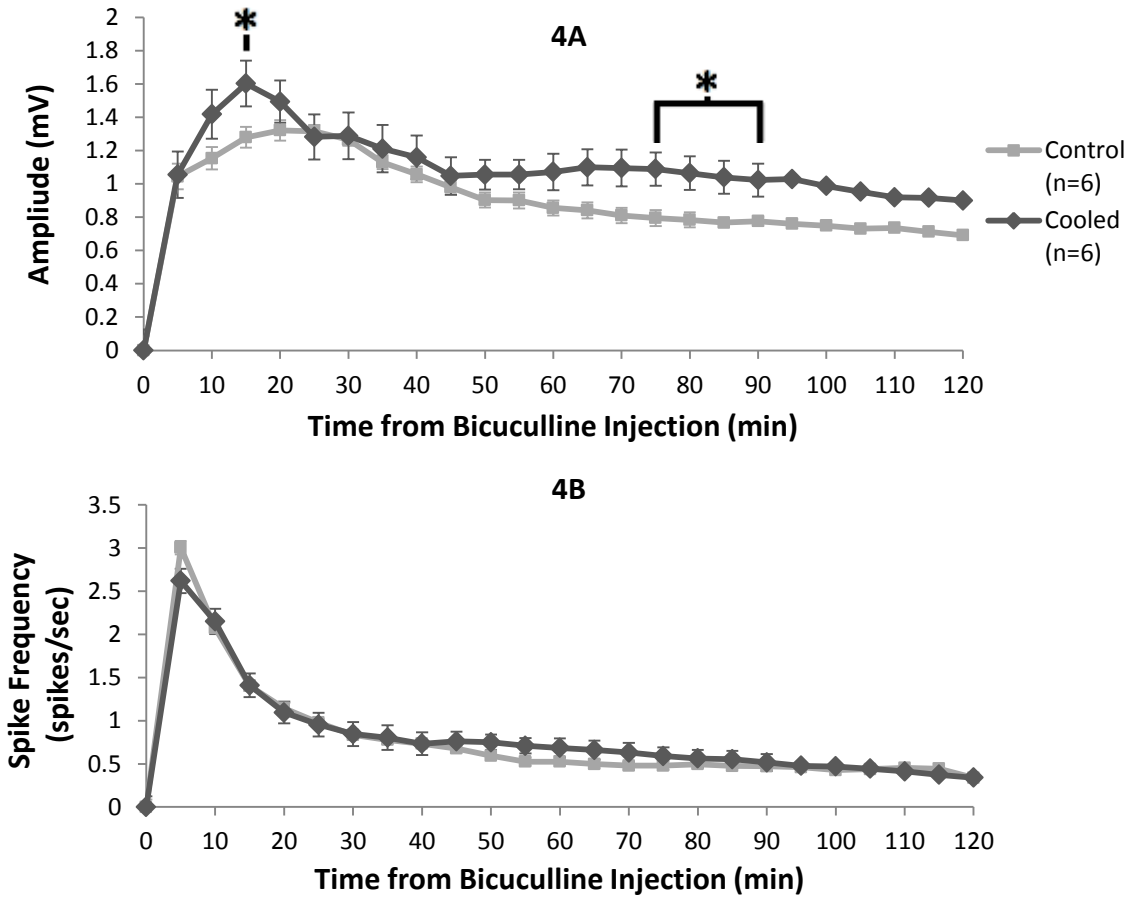

Figure 4. Effects of head cooling on mean ECoG amplitude (A) and spike frequency (B) during bicuculline-induced seizures. Values are means ± SE. * p<0.05.

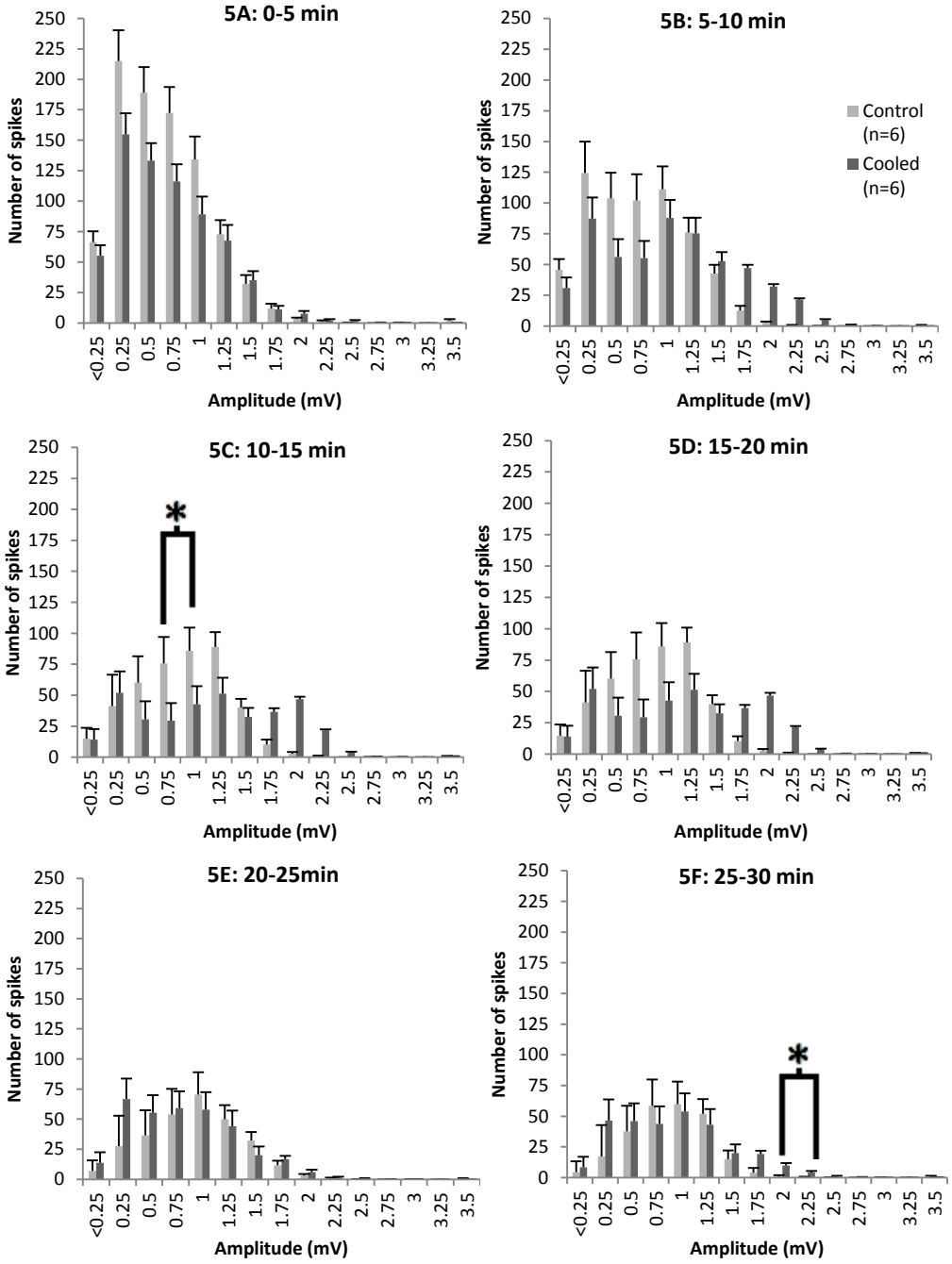

Figure 5. Comparison for mean seizure spike amplitude distribution among cooled and control groups for 0-5 min (A), 5-10 min (B), 10-15 min (C), 15-20 min (D), 20-25 min (E), and 25-30 min (F) after seizure onset. Values are mean ± SEM. * p<0.05.

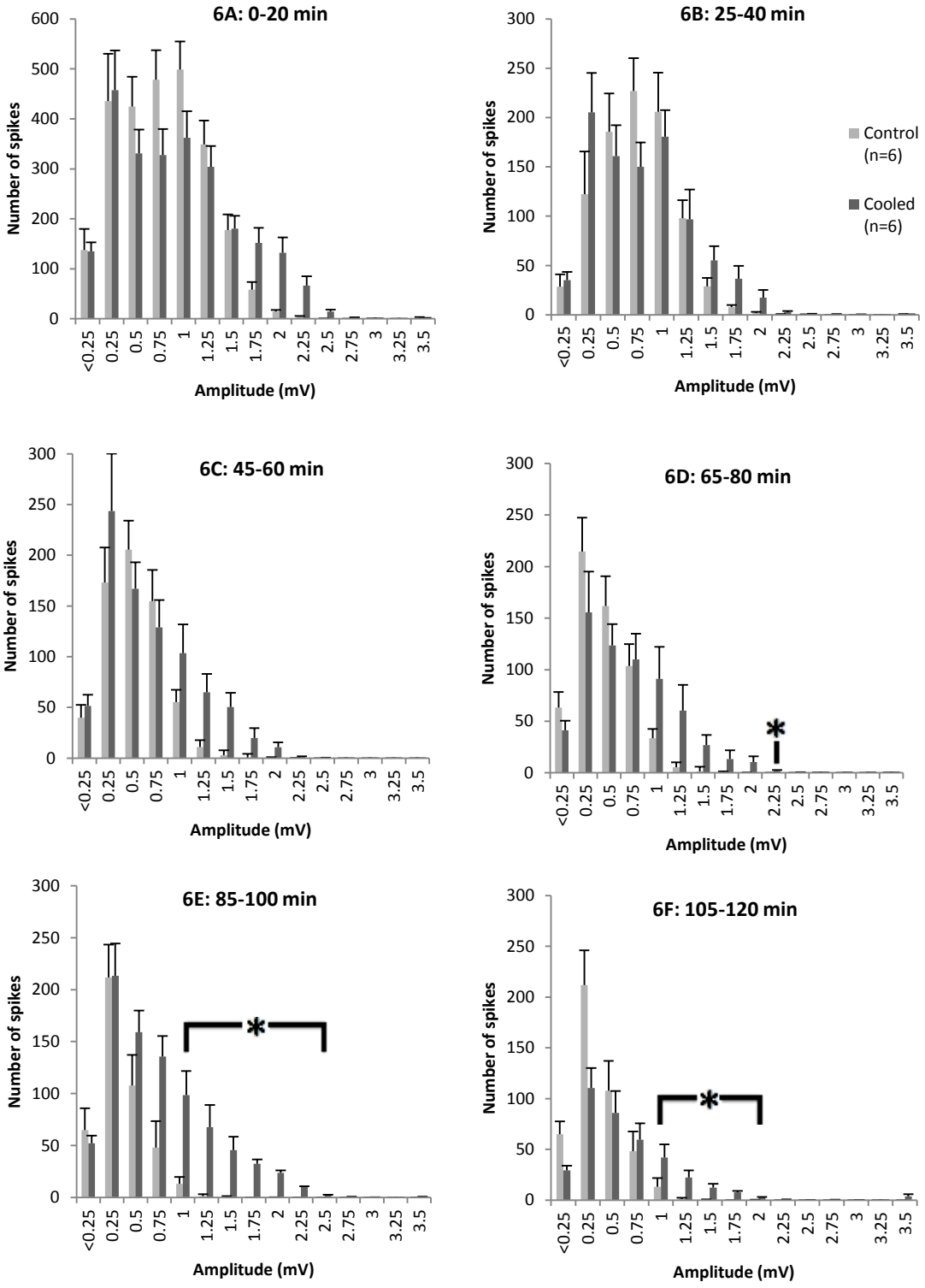

Figure 6. Comparison between mean seizure spike amplitude distributions among cooled and control groups for 0-20 min (A), 25-40 min (B), 45-60 min (C), 65-80 min (D), 85-100 min (E), and 105-120 min (F) after seizure onset. Values are mean ± SEM. * p<0.05.

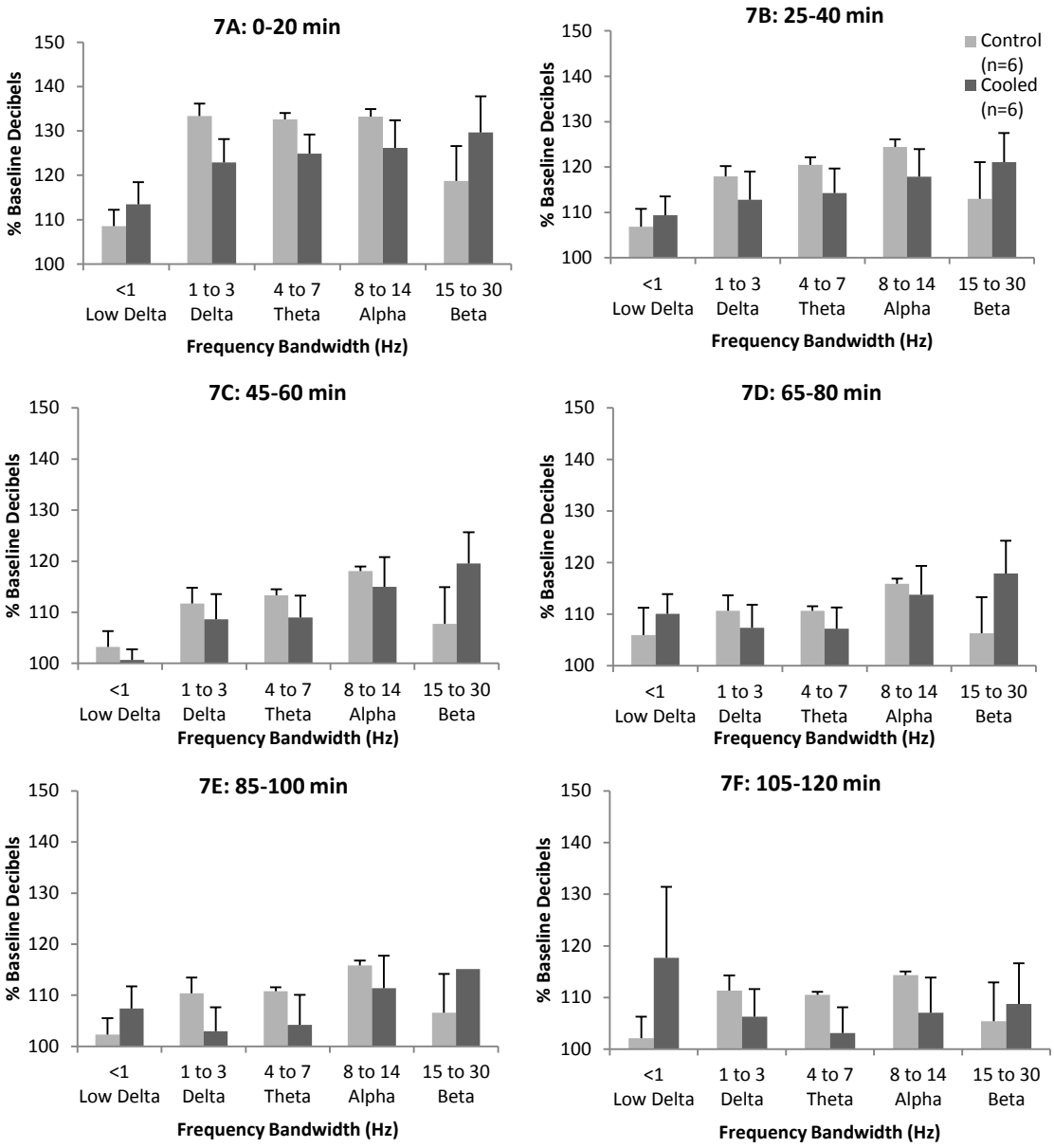

Figure 7. Comparison among cooled and control groups for power distribution in frequency bandwidths after seizure onset for 0-20 min (A), 25-40 min (B), 45-60 min (C), 65-80 min (D), 85-100 min (E), and 105-120 min (F).

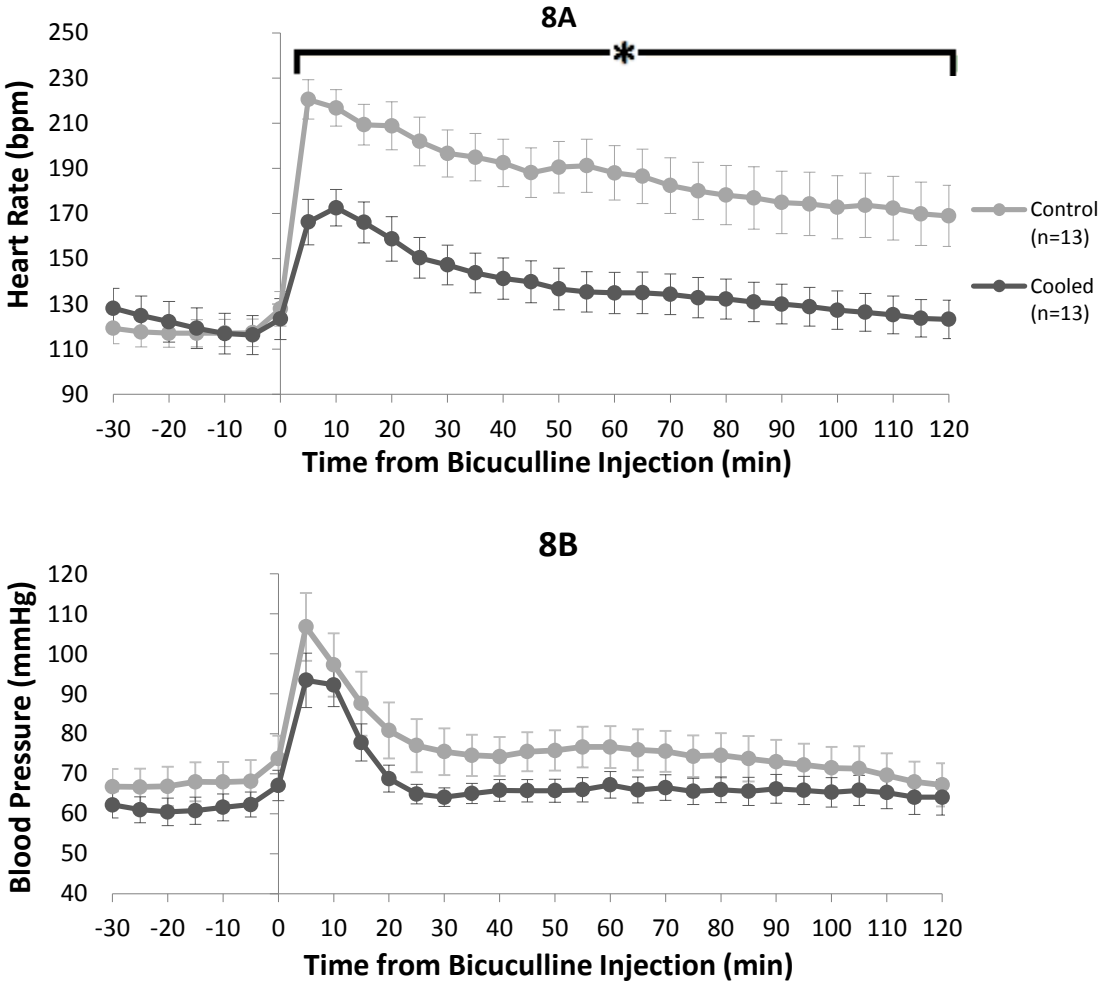

Figure 8. Effects of head cooling on heart rate (A) and MABP (B) before and during seizures. Values are means ± SE. * p<0.05.

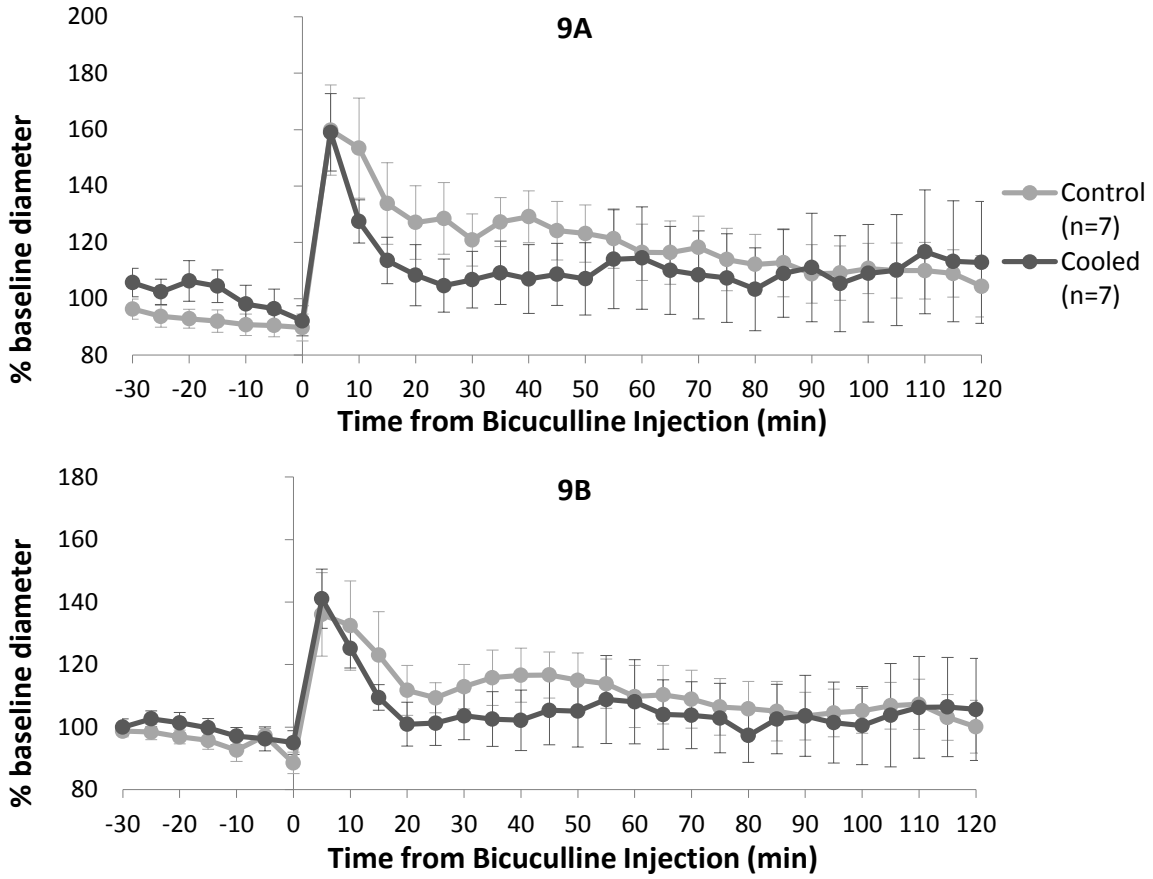

Figure 9. Effects of head cooling on small (A) and large (B) pial arterioles before and during seizures. Values are means ± SE.

Table 1: P-values from statistical comparison between control and cooled groups of seizure spike amplitude distribution over initial 30 minutes post-bicuculline (Welch's t-test α=0.05)

Spike Amplitude Bin (mV)	0-5 min	5-10 min	10-15 min	15-20 min	20-25 min	25-30 min
0.00 – 0.25	0.599	0.434	0.929	0.462	0.207	0.214
0.25 – 0.50	0.239	0.505	0.781	0.582	0.184	0.078
0.50 – 0.75	0.093	0.214	0.152	0.656	0.214	0.609
0.75 – 1.00	0.082	0.118	0.046	0.125	0.736	0.380
1.00 – 1.25	0.164	0.402	0.036	0.072	0.650	0.757
1.25 – 1.50	0.852	0.952	0.219	0.198	0.762	0.649
1.50 – 1.75	0.863	0.590	0.686	0.523	0.536	0.590
1.75 – 2.00	0.941	0.129	0.139	0.569	0.671	0.174
2.00 – 2.25	0.305	0.137	0.165	0.167	0.632	0.115
2.25 – 2.50	0.723	0.201	0.203	0.159	0.669	0.048
2.50 – 2.75	0.271	0.153	0.185	0.171	N/A	0.015
2.75 – 3.00	0.233	0.237	0.372	0.403	N/A	0.107
3.00 – 3.25	0.625	0.431	0.431	N/A	0.372	N/A
3.25 – 3.50	N/A	N/A	N/A	N/A	N/A	N/A
>3.50	0.367	0.363	0.325	0.413	N/A	0.523

Table 2: P-values from statistical comparison between control and cooled groups of seizure spike amplitude distribution over 2 hour post-bicuculline (Welch's t-test α=0.05)

Spike Amplitude bin (mV)	0-20 min	25-40 min	45-60 min	65-80 min	85-100 min	105-120 min
0.00 – 0.25	0.951	0.746	0.620	0.506	0.493	0.239
0.25 – 0.50	0.892	0.303	0.539	0.501	0.895	0.180
0.50 – 0.75	0.264	0.664	0.509	0.372	0.472	0.576
0.75 – 1.00	0.124	0.201	0.645	0.894	0.057	0.589
1.00 – 1.25	0.130	0.719	0.119	0.149	0.003	0.005
1.25 – 1.50	0.553	0.977	0.058	0.106	0.002	0.004
1.50 – 1.75	0.964	0.357	0.119	0.153	0.022	0.009
1.75 – 2.00	0.141	0.293	0.208	0.289	0.009	0.011
2.00 – 2.25	0.067	0.362	0.321	0.388	0.005	0.003
2.25 – 2.50	0.117	0.430	0.363	0.349	5.592E-05	0.026
2.50 – 2.75	0.065	0.654	0.363	0.028	0.004	N/A
2.75 – 3.00	0.107	0.363	N/A	0.865	0.112	0.333
3.00 – 3.25	0.423	0.363	N/A	N/A	0.212	N/A
3.25 – 3.50	N/A	N/A	N/A	N/A	N/A	N/A
>3.50	0.635	0.769	N/A	0.638	0.142	0.425

Table 3: P-values from statistical comparison between power distributions of frequency bandwidths for cooled (n=6) and control (n=6) groups

Bandwidth	**0-20 min**	**25-40 min**	**45-60 min**	**65-80 min**	**85-100 min**	**105-120 min**
<0.5 Hz	0.356	0.522	0.569	0.456	0.267	0.287
0.5 - 3 Hz	0.126	0.362	0.531	0.513	0.189	0.303
4 - 7 Hz	0.123	0.246	0.301	0.364	0.196	0.181
7 - 14 Hz	0.246	0.270	0.465	0.566	0.385	0.289
15 - 30 Hz	0.415	0.449	0.260	0.271	0.412	0.807